DAMPING IN NAILED JOINTS OF LIGHT-FRAME WOOD BUILDINGS[1]

Anton Polensek and Kenneth M. Bastendorff

Professor/Research Engineer and Technician
Department of Forest Products, Oregon State University
Corvallis, OR 97331

(Received August 1985)

ABSTRACT

Nail joints are not only the main source of damping in light-frame wood buildings during earthquakes, but also provide the composite stiffness and strength. Twenty-one joint types with 15 specimens each were tested under fully reversed cyclic loading to characterize the damping and stiffness of typical construction joints. Generally, both properties decrease as the load increases. Among construction variables, lumber species affect these properties the most; the damping ratios of joints between Engelmann spruce and plywood are from 10% to 15%, while the corresponding values for Douglas-fir and western hemlock are from 20% to 40%. Other significant variables include angle between shear force and lumber grain, sheathing material, nail size, and surface friction between wood and concrete or steel.

Keywords: Nail joints, damping, stiffness, friction, cyclic loading, lumber, plywood, gypsum wallboard.

INTRODUCTION

The numerous types of nailed joints that connect a light-frame wood building are characterized by grades and species of framing lumber, sheathing materials, types and sizes of nails and other mechanical connectors, and geometry and wood-grain orientation of connected elements. These types can be categorized into three subtypes according to the mode of stress they transfer: shear stress, normal stress introducing gap or nail withdrawal, and normal bearing stress in interlayers of adjacent elements. Other joint types are combinations of lumber and nonwood materials, such as the concrete foundation and the metal plates and hangers connecting framing elements.

The existing literature on nailed joints is limited mostly to their strength with nails driven perpendicular to the grain. The overemphasis on the importance of strength in the past and the large variety of joint-type configurations are the main reasons for the limited information on the properties of nailed joints. Another is their nonlinear behavior, characterized by decreasing joint stiffness and damping as load and slip increase (Foschi and Bonac 1977; Jenkins et al. 1979). Evaluations of joint stiffness are more recent (Wilkinson 1971; Foschi and Bonac 1977). Jenkins et al. (1979) and Polensek (1982) reported on stiffness deterioration from long-term loading, and Chou (1984) evaluated deterioration in strength and stiffness caused by drying of joints assembled from green lumber.

The main source of damping in nailed wood buildings is interlayer friction, because the coefficient of material damping in wood is only 0.35% (Yeh et al.

---

[1] This is paper 2028 of the Forest Research Laboratory, College of Forestry, Oregon State University, Corvallis, OR 97331. Support for this research was provided by the National Science Foundation, Grant No. CEE-8104626.

1971), compared to overall damping of 10% and more in nailed wood systems (Polensek 1975, 1976a). Damping in joints has been evaluated only for those between Douglas-fir lumber and sheathing such as plywood and gypsum wallboard (Yeh et al. 1971; Atherton et al. 1980; Chou 1984).

Traditionally, damping values for earthquake design of building components originate in laboratory and on-site testing (Blume et al. 1961; Polensek 1975, 1976a), but a few theoretical approaches also exist (Brown 1968; Yeh 1971). The experimental values are considered more reliable, because the theoretical predictions lack accuracy and require interlayer characteristics, such as coefficients of friction, which involve complicated testing.

The main objective of this investigation was the evaluation of stiffness moduli and damping ratios for typical joints in light-frame wood buildings. The procedure employed static cyclic testing and was based on concepts found in the traditional determination of structural damping of building components and materials. Other objectives included characterizing the relation between the properties of joint materials and damping and evaluating damping-related friction in contact surfaces between lumber and concrete.

EXPERIMENTAL

Specimen description

ASTM D 1761 (ASTM 1983) provides recommendations only for static tests of wood joints. Therefore, testing arrangements and procedures for dynamic stiffness and damping were developed during initial phases of this investigation. The techniques successfully used by Jacobsen (1960) provided the basis for the procedure in our investigation. Additional methodology came from the ASTM specifications for static tests and from preliminary testing aimed at characterizing structural mechanisms associated with joint behavior in wood buildings. Because the ASTM slip-controlled loading rate of about 0.15 in./min was considered too slow for repetitive, fully reversed cyclic loading, the rate was increased to 1.5 in./min.

Table 1 identifies the composition of specimen samples, each representing a different joint type. Figure 1 depicts the construction and loading of eight basic configurations investigated. The samples illustrate the major types of joints in a typical light-frame wood building, but they include only a few standard materials to keep the amount of testing manageable. The selected materials represent baseline joint types that are presently considered adequate and are commonly found in light-frame wood buildings.

Specimens were constructed from fifteen clearwood lumber sections selected from three groups of 8- to 16-inch-long boards of mixed structural grades. Each group contained either Douglas-fir, hem-fir, or Engelmann spruce boards. Lumber sections were of clearwood to avoid driving the nail into a knot. The selection was based on specific gravity so that the corresponding sample histograms approximately matched those of actual Douglas-fir, western hemlock, and Engelmann spruce lumber (Polensek and Atherton 1976). Because specific gravity affects joint stiffness (Wilkinson 1971), this selection process was expected to produce representative variability in stiffness in each sample.

Sheathing materials were obtained from local lumber retailers. In order to consider the effects of material variation, each sample included an equal amount

TABLE 1. *Composition and number of samples for each joint type.*

Joint type	Sample size	Configuration*	Connected elements: Material† No. 1	Material† No. 2	Size (in. × in. × in.) No. 1	Size (in. × in. × in.) No. 2	Nail size and type
1	14	b	DF	DF	2 × 4 × 8	2 × 4 × 8	16d, common
2	14	a	DF	DF	2 × 4 × 8	2 × 4 × 8	16d, common
3	15	c	PLWD	DF	3/8 × 4 × 10	2 × 4 × 16	6d, box, galvanized
4	15	c	PLWD	WH	3/8 × 4 × 10	2 × 4 × 16	6d, box, galvanized
5	15	c	PLWD	DF	3/8 × 4 × 10	2 × 4 × 16	8d, box, galvanized
6	15	c	GYP	DF	1/2 × 4 × 10	2 × 4 × 16	4d, drywall
7	15	c	GYP	DP	1/2 × 4 × 10	2 × 4 × 16	5d, drywall
8	15	d	PLWD	DF	3/8 × 4 × 10	2 × 4 × 14	6d, box, galvanized
9	15	d	PLWD	DF	3/8 × 4 × 10	2 × 4 × 14	8d, box, galvanized
10	15	d	PLWD	WH	3/8 × 4 × 10	2 × 4 × 14	6d, box, galvanized
11	14	d	GYP	DF	1/2 × 4 × 10	2 × 4 × 10	4d, drywall
12	14	d	GYP	DF	1/2 × 4 × 10	2 × 4 × 10	5d, drywall
13	14	d	PLWD	DF	1/2 × 4 × 14	2 × 4 × 16	8d, box, galvanized
14	15	d	ST	DF	1/16 × 3 × 7	2 × 4 × 16	8d, common
15	14	c	ST	DF	1/16 × 3 × 7	2 × 4 × 16	8d, common
16	14	e	DF	DF	2 × 4 × 8	2 × 4 × 8	—
17	14	f	DF	DF	2 × 4 × 8	2 × 4 × 8	—
18	14	g	DF	C	2 × 4 × 8	1.5 × 6 × 6	—
19	14	h	DF	DF	2 × 4 × 10	2 × 4 × 6	10d, common
20	15	d	PLWD	ES	3/8 × 4 × 10	2 × 4 × 16	6d, box, galvanized
21	15	c	PLWD	ES	3/8 × 4 × 10	2 × 4 × 16	6d, box, galvanized

* Letters indicate configurations in Fig. 1.
† DF = Douglas-fir, PLWD = CDX plywood, WH = western hemlock, ES = Engelmann spruce, GYP = gypsum wallboard, ST = steel plate (strap), C = concrete.

of material from each of three sheets of sheathing. Three sheets were deemed sufficient for evaluating the average properties of joints, because sheathing properties are considerably less variable than those of lumber.

Lumber sections and sheathing materials were conditioned in an environment of 12% equilibrium moisture content for at least 3 months. Periodic moisture content readings were taken to ensure that the material was equilibrated before the specimen assembly. Nails were driven as in building construction: for plywood specimens, the top of the nail head was driven until it was in the plane of the plywood surface; for gypsum wallboard, nail heads were hammered somewhat below the board surface to imitate on-the-site construction practice.

Testing procedures

The mode of specimen loading produced three different testing procedures: shear loading of nailed joints (Fig. 1a, c, d, and h); withdrawal loading of nailed joints (Fig. 1b); and shear loading of joints connected by constant pressure (Fig. 1e–g). Cyclic loading distinguished the first procedure from the second and third, which used noncyclic ramp loading.

Testing arrangements.—Figures 1f and 2 illustrate one of the testing arrangements. The arrangements for joint types 16 and 18 (Fig. 1e and g) and for types 8 through 14 and 20 (Fig. 1f) were modified from those reported by Atherton et al. (1980). The modification reduced the bending moment on the contact surfaces of joints. For types 2 (Fig. 1a), 3 through 7, 15, 19, and 21 (Fig. 1c), Atherton's

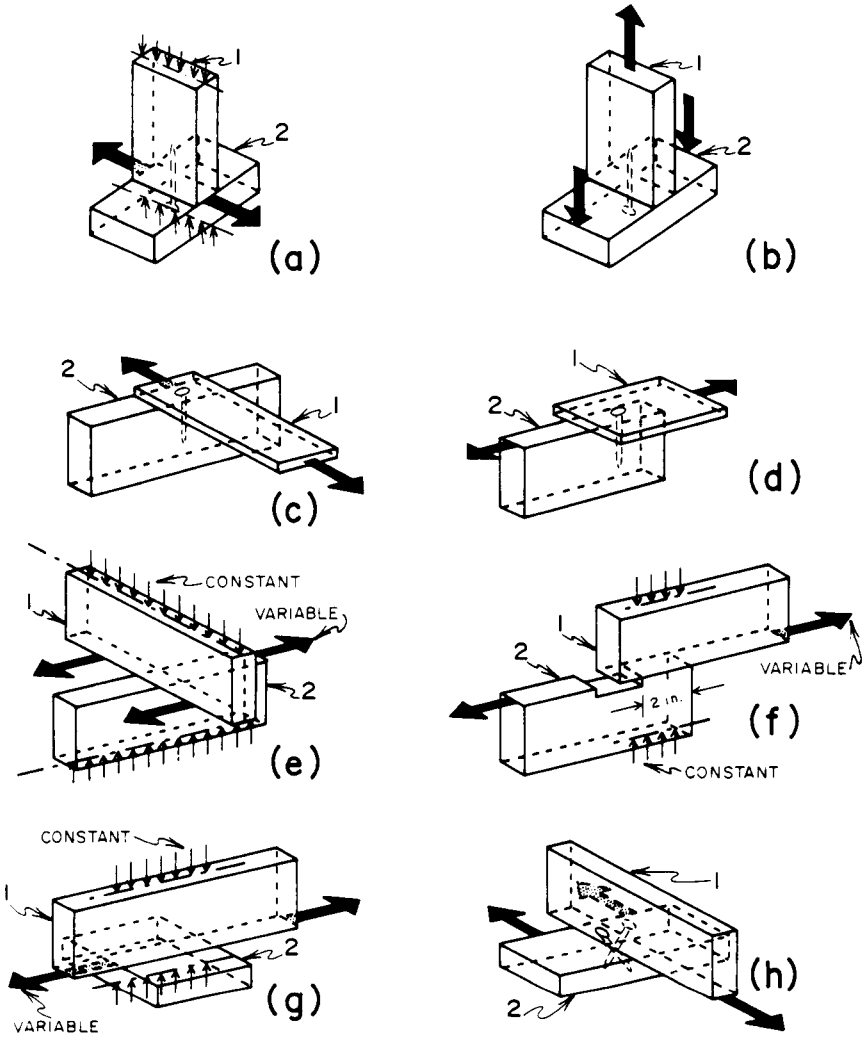

FIG. 1. Basic configurations of joint types.

arrangement was modified to accommodate application of shear force perpendicular to lumber section. The arrangement for nail withdrawal tests (type 1 in Table 1 and Fig. 1b) was two U-shaped steel brackets with their webs attached to the testing machine and flanges to the specimens. The types tested under shear load provided a condition of almost pure shear, as compared to the arrangement recommended by ASTM D 1761 (ASTM 1983) for which the shear is associated with a couple caused by eccentric load application. The shear resistance for most types was provided in the interface by the combination of lateral nail bearing and friction activated by resistance to nail withdrawal. Exceptions were types 16, 17 (Fig. 2), and 18, which had only friction from the normal pressure applied by a hydraulic cylinder mounted at the base of the testing machine.

Loading cycles.—Nail specimens tested in shear were subjected to three cycles of loading and unloading in one direction and then loading and unloading in the

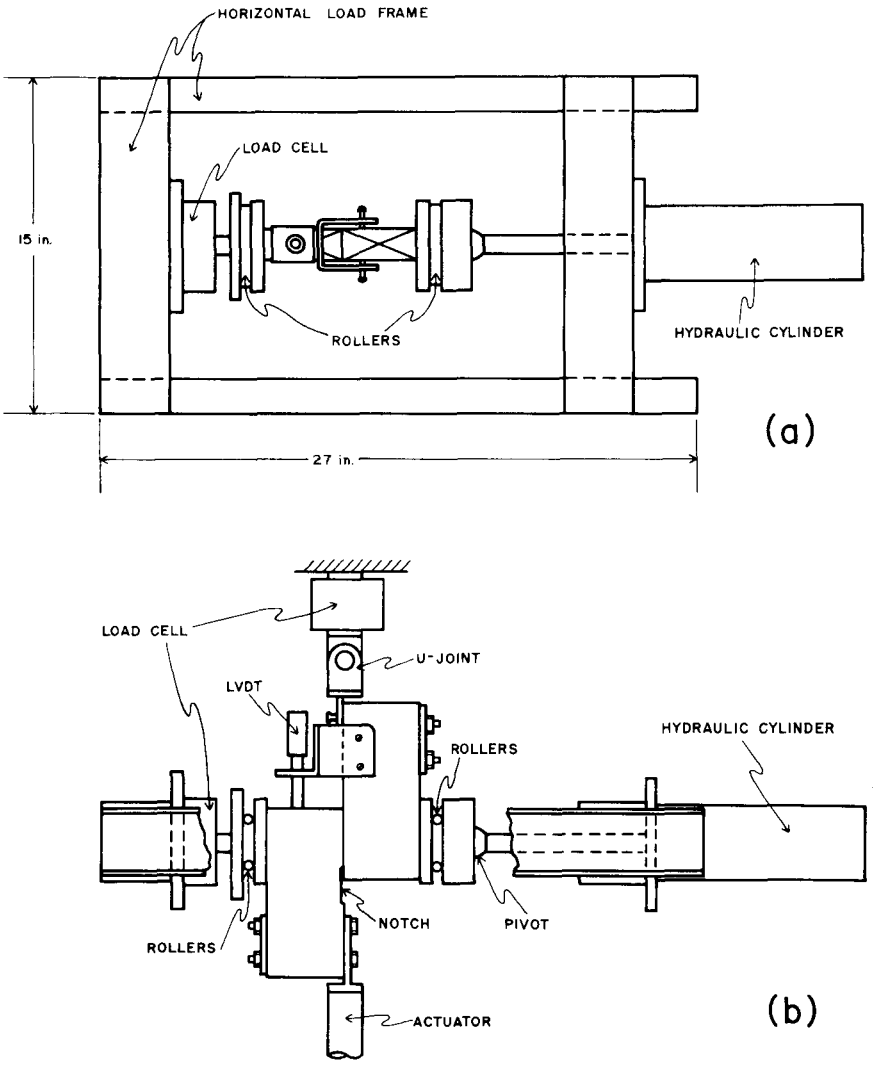

FIG. 2. Testing arrangement for type 17 specimen: (a) top view, (b) side view.

other direction. The cycles were repeated at four progressively larger loads: $\pm P_1$, $\pm P_2$, $\pm P_3$, and $\pm P_4$, where the plus and minus sign denotes the load levels in the two opposite directions. The three cycles were the minimum number that produced an intermediate cycle unaffected by transition from one load level to another (Fig. 3). This minimum number of cycles was selected because Atherton et al. (1980) showed that the ratio between the dissipated and available energy is not affected by the number of cycles. Figure 3 indicates the loading cycles, and the second column of Table 2 lists the levels for individual joint types. The levels were based on data from preliminary testing (Polensek et al. 1984) and existing studies (Atherton et al. 1980; Jenkins et al. 1970) in which a few specimens of each type shown in Table 1 were subjected to a ramp load associated with a constant slip rate of 1.5 in./min, up to a slip of about 0.12 inch. This is the

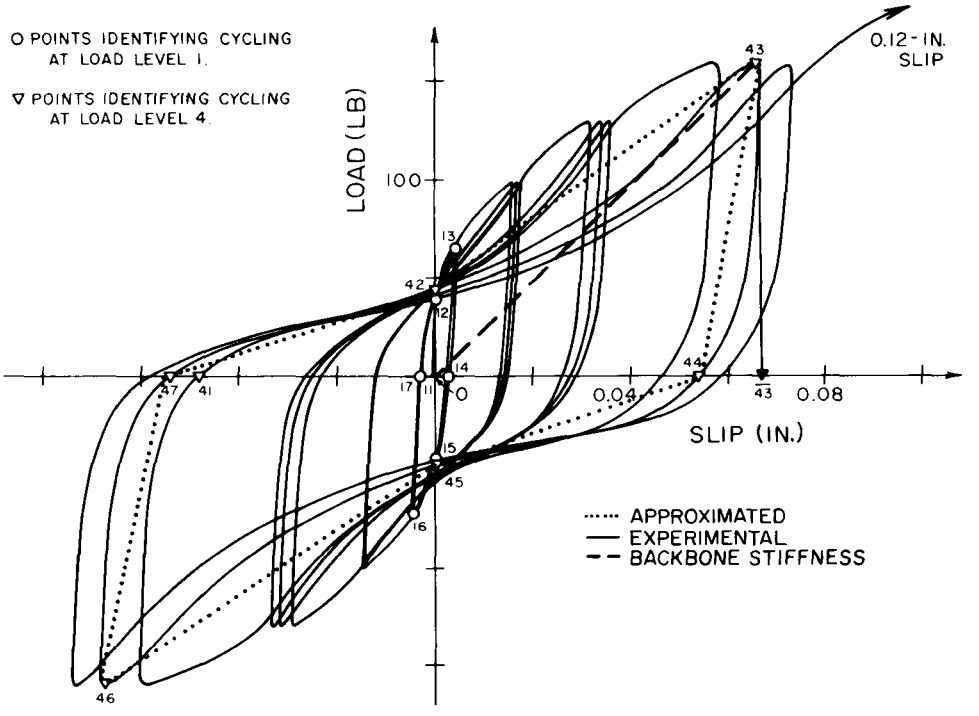

FIG. 3. Points and areas digitized to identify stiffness and damping for cycling at four load levels.

maximum slip expected in bending components such as walls (Polensek 1976b). The load levels were chosen on experimental traces as follows: Four points at locations where the trace slope changed substantially defined four straight lines that represented load-slip traces. For the specimen replications of each type, the loads associated with the first point were averaged to the final given P_1. Levels P_2, P_3, and P_4 were determined in the same way.

Load applications at the slip-controlled rate of 1.5 in./min are about 10 times faster than the slip rate specified by ASTM D 1761 (ASTM 1983). The faster rate was chosen to make the frequency of loading closer to that experienced in actual earthquakes and to decrease the testing time. An investigation on testing speed showed that effects caused by the faster rate could be accounted for by empirically developed correlation factors (Polensek and Laursen 1984).

Type 1 specimens were tested under a constant withdrawal rate of 1.5 in./min until the gap between the two connected pieces reached about 0.12 inch. No reversal loading was attempted, because nails in actual assembly, which pop out under service loads, remain partially withdrawn unless hammered back. In addition, energy dissipation associated with nail withdrawal is very small compared to that of shear slip. Therefore, the reversal stiffness moduli and damping ratios are not needed.

Specimens in types 16, 17, and 18 were subjected to three loading cycles between zero- and 0.12-inch slip. During the first cycle, the side pressure (normal to the joint interface) was 400 psi for types 16 and 17 and 133 psi for type 18. The side pressure was kept constant, while the slip was applied along the interface at a rate

of 1.5 in./min up to the maximum slip of 0.12 inch, then reversed to zero. The side pressure was then released and reapplied to half of its former value, after which the specimens went through the same slip-induced loading and unloading as in the first cycle.

A continuous load vs. slip trace was recorded on an x-y recorder for each specimen. Slip was measured by a linear variable differential transformer attached to both connected elements (Fig. 2). A load cell attached between the testing machine frame and U-joint provided the load signal.

Data reduction and analysis

Digitizing the traces. — Figure 3 shows a typical experimental trace for specimens under fully reversed, triangular loading cycles. The trace is assumed to simulate the load–slip relationship in nail joints of building components during vibration. Therefore, the traces were used to evaluate the representative damping and stiffness values at four levels of the load cycling. The traces were first digitized and then analyzed by the computer. In Fig. 3, the area enclosed by sections 41-42-43-44-41 of the trace represents dissipated work and the area 41-42-43-$\overline{43}$-41 shows total work capacity from combined restoring and damping forces. In evaluation of equivalent viscous damping, the work capacity usually considered is that of area 0-43-$\overline{43}$-0, because in seismic design it is commonly assumed that all of the curve nonlinearity stems from damping and that the restoring force follows linear line 43-0 (Jacobsen 1960). Thus, the areas 41-42-43-44-41 and 0-43-$\overline{43}$-0 were determined by digitizing about 50 to 70 points on each half-cycle of the load vs. slip trace, then computing and accumulating the trapezoidal areas between the two adjacent points. The digitizing was triggered at equal time intervals, so the number of digitized points depended on both the speed of the tracer and the size of the hysteresis loops.

The digitizing was performed for the second cycle of each trace at all load levels and for areas above and below the slip axis. Thus, only one cycle was considered at each level, because the ratio between the dissipated and available energy is the same for all cycles within a level (Atherton et al. 1980). The choice of the second cycle was convenient, because it gave the first complete loop at the load level.

Another aim of digitizing was to identify characteristic points on each load vs. slip trace that would provide the data to define the joint stiffness at individual load levels. For example, on the fourth loop in Fig. 3, the characteristic points are 41 through 47. They were selected at intersections of the trace with both coordinate axes, at maximum loads. Straight lines through these points linearly approximate the load vs. slip relations throughout the cycling at individual levels. The selected points are essential in providing accurate estimates of joint stiffness values for seismic analysis of wood components.

Definition of damping ratio. — The damping ratio for nailed joints is directly related to the energy ratio between the dissipated and corresponding total available energy (Jacobsen 1960; Lazan 1968), which for the k-th loop equals:

$$\lambda_k = D_k/(2\pi U_k) \tag{1}$$

in which λ_k = damping ratio; D_k = dissipated energy; and U_k = available potential energy during cycle k. This equation is also valid for half-loops above and below the slip axis, so that λ for the half-loop above this axis (Fig. 3) equals:

TABLE 2. *Nonlinear stiffness and damping properties of typical nail joints tested under cyclic loading.*

Joint type	Load level (lb)	Coordinates on hysteresis loops*						Damping ratio (%)	
		Slip (0.001 in.)				Load (lb)			
		i3†		i4†		i2†			
		M‡	SD‡	M	SD	M	SD	M	SD
2	130	1.1	0.7	0.5	0.4	76.8	12.7	25.9	13.2
	260	3.0	1.9	1.3	1.0	119.1	32.4	21.1	7.8
	390	5.6	3.0	2.3	1.7	168.0	50.8	17.8	6.3
	520	8.6	4.5	3.3	2.2	224.3	66.7	18.3	6.2
3	70	4.1	2.3	2.2	1.6	32.5	6.1	24.8	2.9
	100	9.2	6.2	5.4	4.1	45.2	9.6	25.2	4.5
	130	22.5	20.7	13.2	14.5	51.9	14.7	22.4	4.7
	160	45.7	35.4	27.6	25.7	52.4	17.0	20.7	4.6
4	70	4.1	1.9	2.3	1.1	34.0	7.3	27.0	5.3
	100	9.2	4.4	5.2	2.3	48.2	10.0	26.4	4.9
	130	19.8	10.5	11.3	5.1	55.5	14.8	24.4	4.9
	160	42.3	26.3	25.1	15.2	58.1	18.3	22.3	4.7
5	110	7.0	3.7	3.7	2.3	48.5	9.7	24.1	3.7
	140	12.1	6.6	6.3	3.2	59.4	12.5	23.1	3.8
	170	20.5	11.6	11.0	5.8	68.4	15.9	22.7	3.5
	200	34.8	20.2	19.6	11.8	69.8	17.5	21.0	3.4
6	15	2.3	0.9	1.0	0.8	5.4	1.8	17.3	7.8
	30	8.1	3.6	4.7	3.4	9.8	2.3	18.7	4.8
	45	23.3	11.9	13.9	7.7	11.8	2.9	18.5	2.7
	60	79.4	42.5	53.8	34.1	13.5	2.3	18.4	11.8
7	15	2.3	1.4	1.0	0.9	5.0	1.2	16.1	4.7
	30	7.3	3.2	4.0	1.8	10.4	3.1	20.5	4.2
	45	18.8	8.8	11.1	4.8	11.7	3.1	18.7	3.5
	60	56.3	30.2	34.3	22.5	12.8	2.0	17.8	1.6
8	70	2.7	1.8	2.3	1.4	48.4	6.9	42.2	9.9
	100	7.8	4.8	6.3	3.5	55.8	10.5	34.8	7.0
	130	18.0	9.8	13.6	6.5	58.0	15.6	29.6	6.0
	160	39.4	27.0	30.7	20.0	58.0	20.0	24.7	5.0
9	110	4.2	2.6	2.8	2.2	70.2	9.1	30.2	3.5
	140	8.0	4.5	5.6	3.7	85.5	13.6	30.0	3.4
	170	14.9	8.0	10.9	5.9	91.7	19.4	29.6	3.8
	200	28.0	215.8	21.2	11.6	92.0	22.3	27.4	4.0
10	70	1.4	0.3	1.1	0.5	48.3	8.5	41.5	10.2
	100	4.2	1.9	3.6	2.0	71.0	6.1	40.4	4.5
	130	11.5	5.1	9.8	12.5	78.6	12.8	35.5	3.9
	160	28.4	14.3	24.2	4.6	75.5	17.7	30.3	4.4
11	15	1.2	1.6	0.9	1.3	6.5	2.2	25.6	12.7
	30	5.5	6.3	4.2	4.7	12.8	4.9	30.8	17.5
	45	21.8	15.3	16.8	10.0	18.7	8.7	27.6	8.2
	60	77.7	21.8	63.3	15.9	16.1	5.7	22.0	4.8
12	15	0.4	0.3	0.3	0.2	8.8	2.7	36.1	12.4
	30	2.5	1.8	2.1	1.6	17.0	4.4	35.8	11.5
	45	11.2	7.6	8.8	5.1	20.0	5.6	29.6	5.9
	60	44.3	15.4	32.4	11.3	17.7	3.8	23.2	5.1
13	110	4.7	3.6	3.7	2.7	61.1	9.3	33.6	5.7
	140	9.6	6.7	7.1	4.4	68.6	13.0	29.5	5.2
	170	17.5	13.3	12.7	9.2	71.5	17.5	26.2	4.7
	200	28.2	20.3	19.9	13.7	69.7	18.9	23.1	4.3

(Table 2 continued on next page)

TABLE 2. *Continued.*

Joint type	Load level (lb)	Coordinates on hysteresis loops*							
		Slip (0.001 in.)				Load (lb)		Damping ratio (%)	
		i3†		i4†		i2†			
		M‡	SD‡	M	SD	M	SD	M	SD
14	100	4.5	1.6	3.0	1.1	48.3	6.3	30.3	4.2
	167	12.2	3.8	6.3	2.3	49.4	44.6	21.0	3.3
	234	27.6	9.0	14.4	5.5	45.3	13.2	15.7	2.2
	300	53.8	20.2	34.1	14.5	50.2	12.3	13.9	1.5
15	100	2.4	0.5	0.5	0.2	21.1	6.7	12.0	2.8
	167	5.0	1.5	1.3	0.8	43.0	13.1	13.1	3.7
	234	8.9	3.2	3.0	1.7	67.2	11.8	15.2	2.6
	300	16.2	5.9	6.4	3.3	83.0	20.8	15.7	2.5
19	130	3.8	1.3	1.6	0.6	48.5	12.3	20.8	4.8
	260	13.1	3.9	4.2	1.1	66.2	15.4	15.7	2.9
	390	33.7	9.8	9.0	2.3	71.6	16.3	12.9	1.6
	520	86.8	38.6	32.6	26.6	84.7	17.9	13.5	2.3
20	70	3.7	1.9	0.3	0.2	41.0	6.5	13.7	1.1
	100	9.3	3.4	0.7	0.2	52.3	10.5	14.4	0.6
	130	24.8	9.2	1.8	0.7	52.3	13.7	14.5	0.4
	160	67.3	26.1	5.1	1.9	43.3	12.6	14.5	0.4
21	70	0.8	0.3	0.4	0.2	24.2	4.0	11.1	1.5
	100	1.9	0.7	0.9	0.4	33.6	6.6	11.8	0.6
	130	5.4	3.1	2.9	2.1	32.7	10.2	12.4	0.8
	160	13.5	8.7	8.5	6.8	30.2	11.6	13.0	0.7

* Identified in Fig. 6.
† i = order of load level; 2, 3, and 4 = positions on hysteresis loops.
‡ M = mean, SD = standard deviation.

$$\lambda_4 = (\text{Area } 41\text{-}42\text{-}43\text{-}44\text{-}41)/[2\pi(\text{Area } 0\text{-}43\text{-}\overline{43}\text{-}0)]; \quad (2)$$

the symbols are defined in Fig. 3. An improved estimate of λ for level 4 is the average of λ above and below the slip axis. Therefore, these averages were evaluated for all the cycles and load levels.

Statistical analysis.—A standard computerized package (Nie et al. 1975) assisted with the statistical analyses. In addition to basic parameters such as mean and standard deviation of individual types, regression relations were investigated for those variables that could logically coexist within the spectrum of experimental conditions. For example, relations accounting for changes in nail size and sheathing thickness were studied, but only for the types tested under the same load function.

RESULTS AND DISCUSSION

Stiffness and damping under cyclic loading

Symmetry of experimental traces.—Figure 3 shows a typical experimental trace of types 3 through 16, 21, and 22. Most traces are approximately symmetric with respect to load and slip axes, but some displayed larger slips to the right or left of the coordinate origin. One possible reason for nonsymmetry is the larger percentage of dense summerwood on one side of the nail than the other. Another is prestressing induced to one side of the joint during nail driving and the subsequent release of the stresses during testing. Although the nonsymmetry had no effect on

TABLE 3. *Regression equations for predicting points that approximate hysteresis loops and damping ratio.*

Joint type	Slip, s_{i4}*				Load, P_i†				Damping ratio‡			
	a × 10^3	b	c × 10^4	r (%)	d	e	f	r (%)	g	h	k × 10^3	r (%)
2	0	0.399	NS§	88	24.4	5,450	0.297	81	0.282	NS	−0.226	33
3	24	0.697	0.401	98	6.2	1,400	0.418	78	0.254	−1.04	NS	60
4	2	0.574	NS	99	2.6	−684	0.570	86	0.280	−1.57	NS	62
5	2	0.557	NS	98	0.7	−730	0.488	76	0.246	−1.17	NS	50
6	1	0.770	−1.450	99	3.6	NS	0.173	77	NS	NS	NS	NS
7	13	0.697	0.929	99	3.8	NS	0.166	72	NS	NS	NS	NS
8	5	0.752	NS	99	22.4	−674	0.387	76	0.497	−1.86	−1.201	73
9	2	0.752	NS	99	5.7	−1,520	0.651	89	0.316	−1.69	NS	58
10	1	0.861	NS	99	4.5	−1,260	0.676	88	0.411	−3.68	NS	63
11	1	0.758	0.908	99	−3.8	−258	0.655	84	0.296	−1.16	NS	33
12	3	0.722	NS	99	2.4	−310	0.493	82	0.353	−2.80	NS	52
13	7	0.679	NS	99	36.0	−471	0.122	53	0.367	NS	0.198	44
14	13	0.644	NS	98	36.0	−471	0.122	53	0.367	NS	0.198	44
15	8	0.443	NS	94	−19.2	1,810	0.461	89	0.102	NS	0.198	44
19	1	0.597	0.499	97	39.0	NS	0.091	65	0.235	0.51	0.303	69
20	2	0.732	NS	99	18.9	−477	0.355	66	0.130	NS	0.129	37
21	10	0.752	−1.627	99	12.2	1,107	0.207	60	0.100	NS	0.164	62

* Equation for slip (in.): $s_4 = a + bs_3 + cP_3$, (s_3, s_4, and P_3 identified in Fig. 3, r = correlation coefficient).
† Equation for load (lb): $P_2 = d + es_3 + fP_3$.
‡ Equation for damping ratio: $\lambda = g + hs_3 + kP_3$.
§ NS = not statistically significant at $\alpha = 0.05$.

damping ratios, it required an alternative procedure to select points 42 and 45 (Fig. 3). The selection consisted of translating the load axis from the initial zero-slip position to a half-point between the slip at points 41 and 44. The intersections of the new load axis with the test trace were the selected points 42 and 45.

Table 2 lists means and standard deviations of results from tests of 17 typical joint configurations. The results were obtained by averaging the corresponding symmetric values above and below the slip axis and using these averages to obtain the sample means and standard deviations.

There are several reasons for accepting and applying results based on trace symmetry above and below the slip axis. The first is that energy values of traces above and below the slip-axis are statistically the same (Atherton et al. 1980). The second is the symmetric appearance of most experimental slip-load traces. Symmetric data are used in the theoretical analysis of wood systems, which calls for changing the damping ratio and stiffness modulus of the system in response to shear load in nail joints. Thus, for a nonsymmetric hysteresis loop, such changes would occur every half-cycle, which would increase the complexity and cost of the analysis.

The data from this investigation provided additional justification for averaging the symmetric traces. A statistical t-test was conducted at the 95% level of significance to determine if the sample means of variables P_i (i = order of load level), s_{i3} (slip at maximum load per cycle), s_{i4} (slip at zero load during load reversal), and the damping ratio for the traces above the slip-axis were equal to the corresponding values for the traces below the axis. The results showed that most variables were equal, with a few exceptions. In type 2, s_{i3} and s_{i4} were different from their symmetric mates, possibly because of "sticking" from the end grain

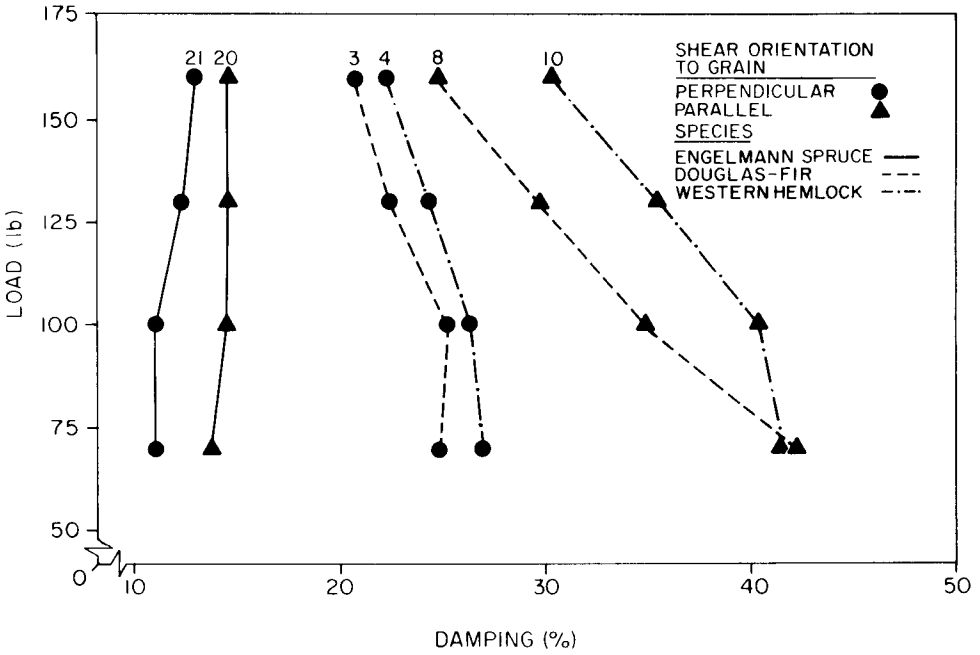

FIG. 4. Effect of species and grain orientation on damping of joints between plywood and lumber. Numbers indicate joint types shown in Table 1.

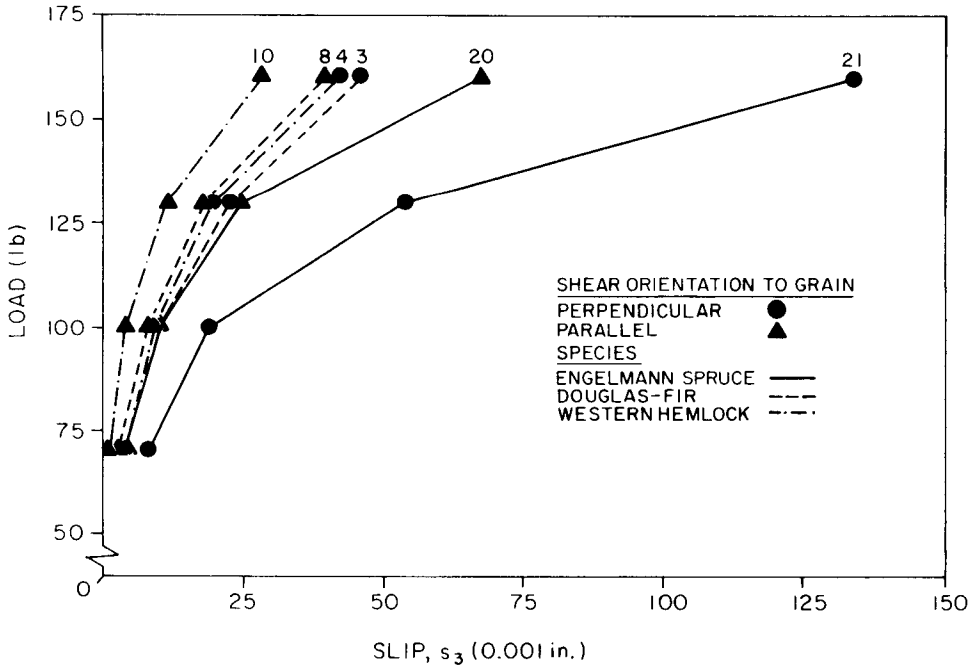

FIG. 5. Effect of species and grain orientation on stiffness of nailed joints between plywood and lumber. Numbers indicate joint types shown in Table 1.

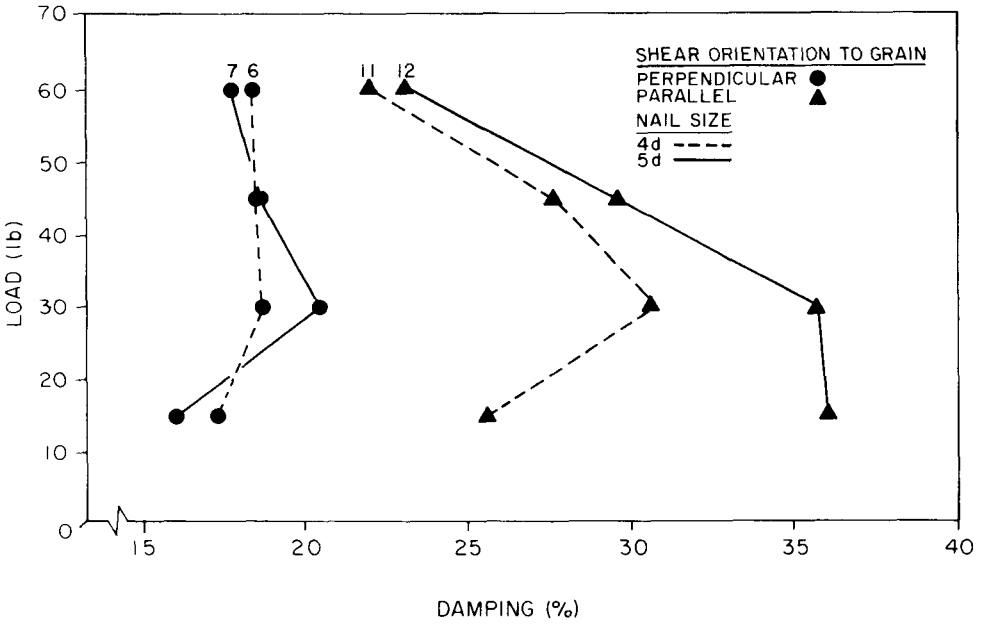

FIG. 6. Effect of grain orientation and nail size on damping of nailed joints. Numbers indicate joint types shown in Table 1.

of studs bearing on the side grain of plates. Additional exceptions were types 5, 13, and 14, which displayed nonsymmetry for several variables at third (i = 3) and fourth (i = 4) load levels. Because these types had 8d nails, rather than the smaller 6d nails used in types 4 and 8, which were symmetric, possibly the larger nail size produced the nonsymmetry. However, this observation is not conclusive, because other variables for samples 5, 13, and 14 tested the same. The overall conclusion is that most traces appear to be symmetric and that averaging the data above and below the slip axis is justified.

Characterization of hysteresis traces.—Points ij (i = 1, 2, 3, 4 for load level and j = 1, 2, . . . , 6 for point on loop) are the characteristic points on the hysteresis loop and define six straight lines that closely represent experimental loops (dotted lines in Fig. 3). To define the whole loop, only four values are needed: slip at i4 (s_{i4}), load at i2 (P_{i2}), and slip and load at i3 (s_{i3} and P_{i3}). Therefore, only these values are shown in Table 2.

Traditionally, most tests on nail joints have been performed under unidirectional ramp load according to ASTM D 1761 (ASTM 1983), which produces only a backbone load-slip trace that is unsuitable for evaluation of the hysteresis loop or damping ratio. Therefore, through statistical regression analyses on the data summarized in Table 2, linear regression equations were developed to relate coordinates of any point on the backbone trace (s_3, P_3) to s_4, P_4, and damping ratio (Table 3). In Table 3, subscript i is omitted from s and P, because P_3 and s_3 are independent variables that denote any point on the backbone trace, and the numbering of loading cycles is no longer necessary. These equations represent the high degree of linear association between slips at s_3 and s_4 as demonstrated by correlation coefficients (r) that are close to 1.0.

TABLE 4. *Effect of individual construction variables on slip and damping ratio at different cycling levels.*

Joint types*	Variable	Slip, s_3†			Damping ratio		
		Specimen type	Level	Interaction	Specimen type	Level	Interaction
3, 4	Species	No‡	Yes	No	No	Yes	No
8, 10	Species	No	Yes	No	Yes	Yes	No
20, 21	Orientation	Yes‡	Yes	Yes	Yes	Yes	Yes
3, 4, 21	Species	Yes	Yes	Yes	Yes	Yes	Yes
8, 10, 20	Species	Yes	Yes	Yes	Yes	Yes	Yes
3, 8	Orientation	No	Yes	No	Yes	Yes	Yes
5, 9	Orientation	Yes	Yes	No	Yes	Yes	No
6, 11	Orientation	No	Yes	No	Yes	No	No
7, 12	Orientation	Yes	Yes	No	Yes	Yes	Yes
14, 15	Orientation	Yes	Yes	Yes	Yes	Yes	Yes
4, 10	Orientation	Yes	Yes	No	Yes	Yes	No
9, 13	Plywood	No	Yes	No	No	Yes	Yes
6, 7	Nail	Yes	Yes	No	No	Yes	No
11, 12	Nail	Yes	Yes	Yes	Yes	Yes	No

* The types compared are identical except for one variable.
† Identified in Fig. 6.
‡ "No" denotes no effect, "yes" denotes significant effect.

Effect of material properties.—Some of the joint types are not only similar in construction, but have the same loading functions; they differ only in one construction variable (Table 1). For example, types 8, 10, and 20, and types 3, 4, and 21 are of the same construction except for the lumber. Furthermore, the mates in pairs 8 and 3, 10 and 4, 20 and 21 are the same except that the shear force is acting parallel to lumber grain in the first mates and perpendicular in the second mates. Results show that species and force orientation affect damping ratio (Fig. 4) and stiffness (Fig. 5) of nail joints. Effects of grain orientation on damping are large and present in joints with both plywood and gypsum sheathing (Figs. 4 and 6), while effects of nail size (Fig. 6) are smaller and more difficult to ascertain. Therefore, the damping and stiffness data of types which were the same except for one construction variable were statistically compared by analysis of variance. The results identify the groups of joint types in which the means of group mates are significantly different (Table 4). For mates with statistically equal means (α = 0.05), the construction variables compared do not affect the property.

Practical application.—An application of these results would consist of initially identifying a pair of types with the desired construction difference in Table 4. Then the means for these two types, for either damping, load, or slip correction, would be selected from Table 2 and divided to form the ratio to correct for the desired construction change. For example, the correction of damping ratio for joint type 4 with 8d instead of 6d nails would proceed as follows: The mean damping ratios for types 5 and 3 would be selected from Table 2 and divided. The resulting ratio would be the multiplier for correcting the known damping ratio, possibly with lumber of a species other than Douglas-fir, for 8d instead of 6d nails.

Theoretically, the correction procedure outlined is valid only for a first-order interaction and is therefore useless when a higher-order interaction is present. Practically, however, the correction is relatively small and applies only to one of

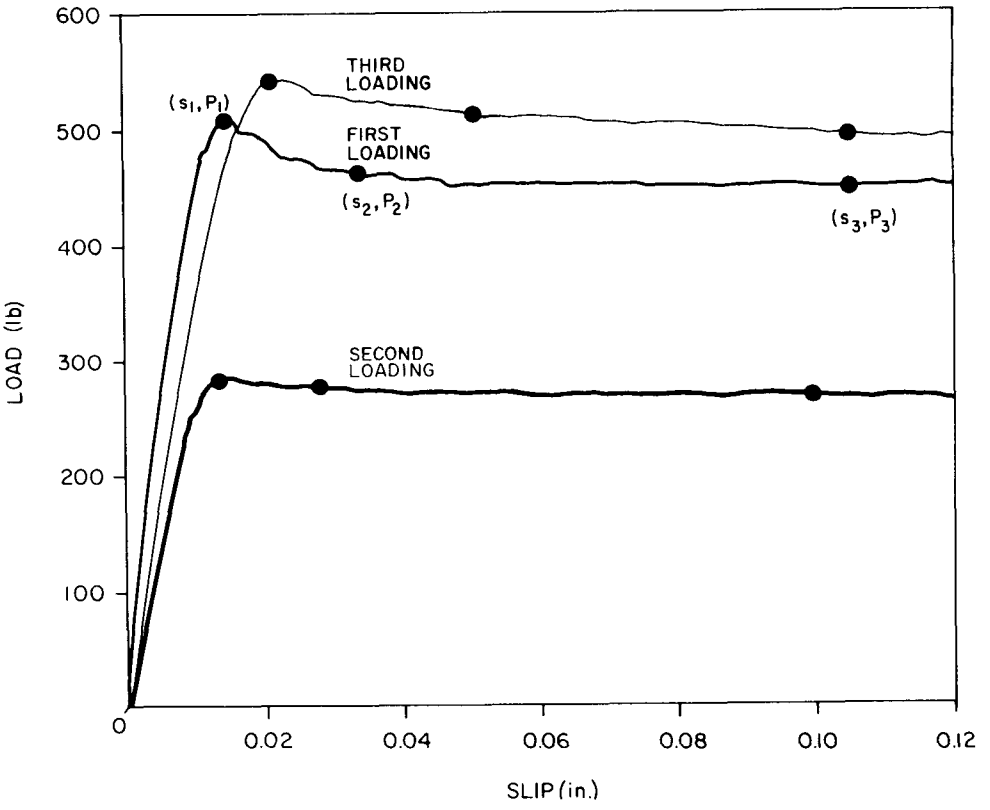

FIG. 7. Typical test traces for type 16 specimens with the points used in a multilinear approximation of traces.

many variables that contribute to total damping or stiffness. A higher-order correction, if the data were available, would normally be only a fraction of a first-order one. Furthermore, no significant higher-order correlation was detected for the variables in Table 4. The correction procedure outlined should, therefore, be reasonably accurate.

Stiffness and interlayer friction under ramp loading

The mechanism of nail withdrawal in type 1 specimens contributed to stiffness and strength but not to damping. Thus, only the coordinates of the characteristic points similar to those of type 16 (Fig. 7) are presented for the traces of withdrawal load vs. separation of connected elements (Table 5). Variables such as withdrawal stiffness and strength can be easily determined from this information.

Specimens in types 16, 17, and 18 were subjected to constant load normal to the contact surface and increasing ramp load. Typical behavior of these joints is characterized by high initial stiffness (Fig. 7) before the connected elements start to slip. The maximum load, usually reached just before the slippage starts, divided by the corresponding constant load normal to the contact surface, defines the coefficient of the static friction. During subsequent slippage, the load is below its maximum value and very slowly decreases, possibly because of the gradual

TABLE 5. *Coordinates defining load-slip traces and coefficient of friction for joint types tested under ramp loading.*

Joint type	Statistics*	Coordinates† for load vs. slip traces‡						Friction coefficients
		s_1	P_1	s_2	P_2	s_3	P_3	
1	M	0.010	188	0.037	159	0.100	154	—
	SD	0.002	86	0.022	62	0.002	63	—
16	M	0.010	465	0.041	423	0.100	417	0.516
	SD	0.003	73	0.013	71	0.000	77	0.081
17	M	0.002	731	0.029	710	0.100	679	0.610
	SD	0.002	72	0.011	76	0.000	66	0.060
18	M	0.001	843	0.021	1,001	0.100	984	0.834
	SD	0.000	76	0.007	65	0.000	73	0.055

* M = mean value of 14 specimens, SD = standard deviation.
† Slip s_i is in inches and load P_i is in pounds (i = order of loading).
‡ Identified in Fig. 7.

smoothing of the contact surfaces. Table 5 shows the mean values of the characteristic coordinates that identify the average trace for joint types tested.

CONCLUSIONS

Results of this study show that typical nailed joints in light-frame buildings not only dissipate energy under earthquake loading, but also contribute to the composite strength and stiffness of buildings. Damping and stiffness properties defining hysteresis loops that relate load and slip at four levels of shear load can be applied in the theoretical analysis of building systems. A methodology of such an application can be in a form of equivalent energy dissipation (Lazan 1968; Polensek 1984). Damping ratios varied between 10% and 40%, depending on the specimen construction and load level. The properties were highly nonlinear, with damping ratios and joint stiffness usually getting smaller under increasing load. Therefore, the theoretical analysis of wood systems cannot be accurate unless it includes nonlinear modeling for joint damping and stiffness.

Lumber species affected damping and stiffness most. The damping ratios of joints between Engelmann spruce and plywood sheathing are between 10% and 15%, while the corresponding values for Douglas-fir and western hemlock specimens are between 20% and 40%. Other construction variables that significantly affected joint properties are the angle between the lumber grain and shear load, sheathing material, and nail size. The results also show that bearing surfaces have the coefficient of static friction between 0.52 and 0.61 for lumber to lumber joints and 0.83 for wood to concrete joints, which indicates that these surfaces can dissipate significant amounts of dynamic energy as well as resist shear.

REFERENCES

AMERICAN SOCIETY FOR TESTING AND MATERIALS. 1983. Annual book of standards, volume 04.09, wood. ASTM, Philadelphia, PA.

ATHERTON, G. H., K. E. ROWE, AND K. M. BASTENDORFF. 1980. Damping and slip of nailed joints. Wood Sci. 12(4):218.

BLUME, J. A., R. L. SHARPE, AND E. ELSESSER. 1961. A structural-dynamic investigation of fifteen school buildings subjected to simulated earthquake motion. Report prepared for the State of California, Department of Public Works, Division of Architecture, Sacramento, CA.

BROWN, C. B. 1968. Factors affecting the damping of a lap joint. J. Struct. Div., ASCE 94(ST5): 1197.

CHOU, C. 1984. Effect of drying on damping and stiffness of nailed joints between wood and plywood. M.S. thesis, Department of Forest Products, Oregon State University, Corvallis, OR.

FOSCHI, R. O., AND T. BONAC. 1977. Load-slip characteristics for connections with common nails. Wood Sci. 9(3):118.

JACOBSEN, L. S. 1960. Damping in composite structures. Proceedings of the Second World Conference on Earthquake Engineering, Tokyo, Japan.

JENKINS, J. L., A. POLENSEK, AND K. M. BASTENDORFF. 1979. Stiffness of nailed wall joints under short- and long-term lateral loads. Wood Sci. 11(3):145.

LAZAN, B. J. 1968. Damping of materials and members in structural mechanics. Pergamon Press, Inc., New York, NY.

NIE, N. H., C. H. HULL, J. G. JENKINS, K. STEINBRENNER, AND D. H. BENT. 1975. Statistical package for the social sciences. McGraw-Hill, New York, NY.

POLENSEK, A. 1975. Damping capacity of nailed wood joist floors. Wood Sci. 8(2):141.

———. 1976a. Damping of roof diaphragm with tongue and groove decking. Wood Sci. 9(2):70.

———. 1976b. Finite element analysis of wood stud walls. J. Struct. Div., ASCE 102(ST7):1317.

———. 1982. Creep prediction for nailed joints under constant and increasing loading. Wood Sci. 15(2):183.

———. 1984. Nonlinear damping in nailed wood components. Pages 301–304 *in* Proceedings, Fifth Engineering Mechanics Division Specialty Conference. American Society of Civil Engineers, New York, NY.

———, AND G. H. ATHERTON. 1976. Compression-bending strength and stiffness of walls with utility grade studs. For. Prod. J. 26(11):17–25.

———, AND H. I. LAURSEN. 1984. Seismic behavior of bending components and intercomponent connections of light frame wood buildings. Report to the National Science Foundation for Grant No. CEE-8104626, submitted by Oregon State University, Corvallis, OR.

WILKINSON, T. L. 1971. Theoretical lateral resistance of nailed joints. J. Struct. Div., ASCE 97(ST5): 1381.

YEH, C. T., G. J. HARTZ, AND C. B. BROWN. 1971. Damping sources in wood structures. J. Sound Vib. 19(4):411.